User-Exposure-Cancelling Beamforming for Multi-Antenna Systems

Miguel R. Castellanos, Borja Peleato, and David J. Love
School of Electrical and Computer Engineering
Purdue University, West Lafayette, IN 47907
castellm@purdue.edu, bpeleato@purdue,edu, djlove@purdue.edu

***Abstract*— Wireless communication systems operating in close proximity to the human body are subject to user electromagnetic absorption regulations. Complying with electromagnetic exposure thresholds will become increasingly difficult as portable devices are equipped with more radios and multiple antennas. Despite these issues, there has been a limited amount of research on the design and analysis of transmission methods incorporating exposure constraints. To address this, we propose a beamforming scheme that leverages existing exposure models for multi-antenna systems to design low-exposure beams which achieve high receive signal-to-noise ratio (SNR). We demonstrate that in exposure-constrained systems, our proposed scheme outperforms traditional power reduction methods.**

I. Introduction

During operation, wireless devices emit electromagnetic (EM) radiation that is partially absorbed by users. While radio frequency (RF) fields are non-ionizing and therefore do not carry sufficient energy to directly alter the structure of DNA, they can induce tissue heating by causing atomic vibration. High exposure levels can lead to biologically significant temperature increases, which can cause pain and even tissue damage [1].

The absorption of EM energy by users is regulated by the Federal Communications Commission (FCC) in the United States and by similar agencies around the world to protect users from high exposure values [2], [3]. A number of dosimetric quantities are employed to quantify RF radiation intensity, and the choice of an appropriate restriction depends on the exposure scenario and the application [4], [5]. Specific absorption rate (SAR), which has units of W/kg and measures power absorbed per unit mass, is the standard measure of electromagnetic exposure for sub-6 GHz systems. At millimeter wave frequencies and beyond, however, electromagnetic radiation is mostly absorbed at the tissue surface and is therefore better characterized by superficial quantities such as incident power density (PD) and SAR at the tissue surface [6]. Regardless of the measure, exposure from wireless devices must lie below regulatory thresholds.

The uplink performance of wireless networks is becoming increasingly exposure-constrained. Exposure standards are typically enforced with regards to *worst-case* exposure, i.e., with the device operating at full power and all transceivers operating simultaneously. Modern devices integrate multiple radios to allow for concurrent communication over various standards, such as Wi-Fi and Bluetooth, and each transceiver increases the maximum potential exposure. For devices operating above 30 GHz, the large antenna arrays employed to overcome high path and blockage losses (see [7], [8], for example) may result in narrow, energy-dense beams directed at the user. Moreover, exposure at these frequencies is largely confined to the tissue surface, which leads to a large amount of energy deposition in the skin and potentially damaging exposure values [6]. Systems that do not proactively manage user exposure must reduce the transmit power to comply with regulations. Therefore, exposure restrictions often act as additional power constraints and can severely limit the system achievable rate.

One key advantage of multi-antenna systems, however, is the ability to vary electromagnetic exposure by adapting the transmit signal. Intuitively, the amount of electromagnetic energy absorbed by users is dependent on the beamformed radiation pattern. Models for exposure in terms of the transmit signal have been investigated and validated in numerous studies [9]–[15]. These models can be incorporated into the device to grant the system exposure-awareness, i.e., the means to calculate the exposure induced by any transmit signal. Recent works have shown success in leveraging signal-level exposure models to design transmission schemes which comply with exposure limits without sacrificing performance [11], [12], [16]–[18].

The aforementioned research related to exposure mitigation via signal design has mainly focused on optimal signaling methods, where the transmit signal maximizes the system throughput under a transmit power constraint and an exposure constraint. While the analyses in [16]–[18] provide insights into the effects of exposure constraints on system performance, the optimal strategies require solving the Lagrange dual problem. These approaches may not be feasible in devices with limited computational power. In addition, the optimal signaling scheme requires channel knowledge at the transmitter, which may not be readily available.

In this paper, we leverage existing signal-level exposure models to develop a low-complexity exposure reduction scheme. Rather than reducing the transmit power of a given beamforming vector to comply with exposure limits, we apply a small perturbation to the beamformer, where the perturbation size is chosen so that the resulting beamformer complies with the exposure constraint. We show that the resulting beam-

This work was supported in part by the National Science Foundation under grant CNS-1642982.

former can be viewed as the sum of the original beam with reduced power and an orthogonal component which mainly acts to decrease exposure. In contrast to optimal exposure-constrained beamforming, the proposed approach does not require channel knowledge and can be performed offline. Our simulation results demonstrate that the proposed approach outperforms traditional power back-off methods.

Notation: A bold lowercase letter $\mathbf{a}$ denotes a column vector, a bold uppercase letter $\mathbf{A}$ denotes a matrix, $\mathbf{A}^T$ denotes the transpose of $\mathbf{A}$, $\mathbf{A}^H$ denotes the conjugate transpose of $\mathbf{A}$, a_i denotes the ith element of $\mathbf{a}$, and $\|\mathbf{a}\|$ denotes the vector 2-norm of $\mathbf{a}$. $\mathbf{A} = \text{diag}(a_1, a_2, \ldots, a_N)$ denotes the diagonal matrix A with diagonal entries given by $a_1, a_2, \ldots, a_N$. For a complex number z, $\text{Re}(z)$ and $\text{Imag}(z)$ denote the real and imaginary parts of z, respectively.

II. System Model and Motivation

A. System Model

We consider an uplink MIMO system with N_T transmit antennas and N_R receive antennas, where the transmitter operates in the vicinity of the user as seen in Fig. 1. During each transmission, a symbol $s \in \mathbb{C}$ with $\mathbb{E}\left[|s|^2\right] = 1$ is multiplied by the transmit beamforming vector $\mathbf{f} \in \mathbb{C}^{N_T}$ and the receiver observes the output signal $\mathbf{y} \in \mathbb{C}^{N_R}$ given by

$$\mathbf{y} = \mathbf{H}\mathbf{f}s + \mathbf{z}, \tag{1}$$

where $\mathbf{H} \in \mathbb{C}^{N_R \times N_T}$ denotes the channel matrix, and $\mathbf{z} \in \mathbb{C}^{N_R}$ denotes the Gaussian noise vector with i.i.d. entries distributed as $\mathcal{CN}(0, \sigma^2)$.

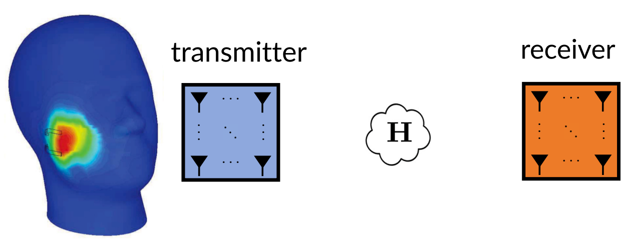

Fig. 1. Diagram of the considered system model, in which a transmitter operating near the user communicates with a receiver in the far-field through the channel $\mathbf{H}$.

The transmitter is assumed to be subject to an exposure constraint due to its proximity to the user. In order to place an exposure constraint on the system, we adopt the quadratic model proposed and validated in [9], [11]–[13], [15]. Here, the instantaneous exposure for a particular volume/gesture can be modeled as

$$\text{EXP} = \mathbf{x}^H \mathbf{R} \mathbf{x}, \tag{2}$$

where $\mathbf{x} = \mathbf{f}s$ is the transmit signal and $\mathbf{R}$ is the characteristic exposure matrix for the volume/gesture. We assume that $\mathbf{R}$ is a Hermitian, full-rank, positive-definite matrix.

Since exposure measurements are time-averaged, the exposure constraint can be expressed as

$$\text{EXP}_{\text{avg}} = \mathbb{E}\left[\mathbf{x}^H \mathbf{R} \mathbf{x}\right] = \mathbf{f}^H \mathbf{R} \mathbf{f} \leq Q, \tag{3}$$

where Q is the regulatory exposure threshold. Note that the quadratic model in (2) is applicable for both SAR and incident PD. In addition, $\mathbf{R}$ can be chosen to correspond with the worst-case volume and gesture.

We consider the problem of maximizing the achievable rate of the system for a given channel realization under both a power constraint and an exposure constraint, which can be formulated as

$$\begin{aligned} \max_{\mathbf{f}} \ & \log\left(1 + \frac{1}{\sigma^2}\|\mathbf{H}\mathbf{f}\|^2\right) \\ s.t. \ & \mathbf{f}^H \mathbf{f} \leq P, \\ & \mathbf{f}^H \mathbf{R} \mathbf{f} \leq Q. \end{aligned} \tag{4}$$

B. Prior Work

The most commonly employed method for handling exposure limitations is known as power back-off, in which the transmit power is reduced to comply with exposure regulations. The beamformer $\mathbf{f}$ is chosen according to the desired criteria but without consideration of the exposure constraint, and the transmitter then beamforms with $\gamma\mathbf{f}$, where $\gamma \in [0, 1]$ is a power back-off factor chosen so that $\gamma^2 \mathbf{f}^H \mathbf{R} \mathbf{f} \leq Q$. Power back-off can be applied solely based on the worst-case exposure or adaptively as a function of the current exposure. In the worst-case scenario, the power back-off factor can be expressed as

$$\gamma_{\text{worst}} = \sqrt{\min\left(1, \frac{Q}{\max_{\mathbf{f}} \mathbf{f}^H \mathbf{R} \mathbf{f}}\right)}, \tag{5}$$

while the adaptive power back-off factor for a given beamformer $\mathbf{f}$ is given by

$$\gamma_{\text{adp}} = \sqrt{\min\left(1, \frac{Q}{\mathbf{f}^H \mathbf{R} \mathbf{f}}\right)}. \tag{6}$$

The scaled beamformer can be shown to satisfy the exposure constraint in both cases, but adaptive back-off achieves better performance since this method only reduces power as needed.

The optimal solution to (4) has also been studied in-depth in [16], where it has been shown the optimal exposure-aware beamforming method is shown to vastly outperform back-off techniques. This work also discusses how to optimally precode multiple data streams under a power constraint and multiple exposure constraints. However, the optimal solution requires solving the dual problem online, which may be computationally intensive and require high power consumption. In addition, such a scheme assumes that the channel is known at the transmitter. Our proposed scheme alleviates both of these problems.

III. Exposure-Cancelling Beamforming

In this section, we design a low-complexity beamforming scheme which achieves a satisfactory trade-off between minimizing exposure and maximizing the system achievable rate. We present a method to modify a beamforming vector to reduce its exposure without significantly affecting the beamforming gain. In other words, our goal is to form a beamformer $\tilde{\mathbf{f}}$ from $\mathbf{f}$ such that $\tilde{\mathbf{f}}^H \mathbf{R} \tilde{\mathbf{f}} \leq Q$ but $\|\mathbf{H}\tilde{\mathbf{f}}\|^2 \approx \|\mathbf{H}\mathbf{f}\|^2$.

Given a beamforming vector $\mathbf{f}$, we consider a perturbation approach in which we set

$$\tilde{\mathbf{f}}_\varepsilon = \mathbf{f} + \mathbf{p}_\varepsilon, \tag{7}$$

where $\mathbf{p}_\varepsilon$ is the perturbation vector with $\|\mathbf{p}_\varepsilon\| \le \varepsilon$, and ε is the maximum perturbation size. The perturbation vector $\mathbf{p}_\varepsilon$ is designed to minimize the exposure within a sphere of radius ε centered at $\mathbf{f}$, and is given by

$$\begin{aligned} \mathbf{p}_\varepsilon = &\operatorname*{argmin}_{\mathbf{p}} \left(\mathbf{f}+\mathbf{p}\right)^H \mathbf{R}\left(\mathbf{f}+\mathbf{p}\right) \\ &s.t. \qquad \|\mathbf{p}\|^2 \le \varepsilon^2. \end{aligned} \tag{8}$$

Note that if $\|\mathbf{f}\|^2 \le \varepsilon$, then $\mathbf{p} = -\mathbf{f}$ is a trivial solution to (8). Therefore, we restrict our choice of ε to the interval $(0, \|\mathbf{f}\|)$.

The problem in (8) is a quadratically-constrained quadratic problem (QCQP) and is therefore convex. The Lagrangian of this problem is given by

$$L(\mathbf{p},\mu) = \left(\mathbf{f}+\mathbf{p}\right)^H \mathbf{R}\left(\mathbf{f}+\mathbf{p}\right) + \mu\left(\mathbf{p}^H\mathbf{p} - \varepsilon^2\right), \tag{9}$$

where μ is the dual variable corresponding to the norm constraint on $\mathbf{p}_\varepsilon$. The following Lemma gives an optimal solution to (8).

Lemma 3.1. *Let $\varepsilon \in (0,\|\mathbf{f}\|)$ and let $\mathbf{R} = \mathbf{V}\mathbf{\Lambda}\mathbf{V}^H$ be the eigendecomposition of $\mathbf{R}$, where $\mathbf{\Lambda} = diag(\lambda_1, \lambda_2, \ldots, \lambda_{N_T})$. Let $\mathbf{D}_\mu = diag(d_1^{(\mu)}, d_2^{(\mu)}, \ldots, d_{N_T}^{(\mu)})$ be a diagonal matrix with entries given by*

$$d_n^{(\mu)} = \frac{1}{1+\mu/\lambda_n}, \quad n = 1,2,\ldots,N_T. \tag{10}$$

If there exists μ such that

$$\varepsilon^2 = \sum_{n=1}^{N_T} \left(\frac{|u_n|}{1+\mu/\lambda_n}\right)^2, \tag{11}$$

where $\mathbf{u} = \mathbf{V}^H\mathbf{f}$, then

$$\mathbf{p} = -\mathbf{V}\mathbf{D}_\mu\mathbf{u} \tag{12}$$

is an optimal solution to (8).

Proof: Since the optimization problem in (8) is convex and satisfies Slater's condition, the Karush-Kuhn-Tucker (KKT) conditions are necessary and sufficient for the optimality of $\mathbf{p}$. These conditions are given as

$$\mathbf{R}\left(\mathbf{f}+\mathbf{p}\right) + \mu\mathbf{p} = \mathbf{0}, \tag{13}$$

$$\mathbf{p}^H\mathbf{p} \le \varepsilon^2, \tag{14}$$

$$\mu \ge 0, \tag{15}$$

$$\mu\left(\mathbf{p}^H\mathbf{p} - \varepsilon^2\right) = 0. \tag{16}$$

Note that if $\mu = 0$, then $\mathbf{f} = -\mathbf{p}$ from (13). However, this is not possible since this implies that $\|\mathbf{e}\|^2 = \|\mathbf{f}\|^2 > \varepsilon^2$, and $\mathbf{p}$ must satisfy (14). Therefore, we conclude that $\mu > 0$.

In the case $\mu > 0$, (13) can be rearranged to give

$$\mathbf{p} = -\left(\mathbf{I}_{N_T} + \mu\mathbf{R}^{-1}\right)^{-1}\mathbf{f}. \tag{17}$$

The matrix inverse in (17) can be further simplified as

$$\begin{aligned} \left(\mathbf{I}_{N_T} + \mu\mathbf{R}^{-1}\right)^{-1} &= \left(\mathbf{V}\mathbf{V}^H + \mu\mathbf{V}\mathbf{\Lambda}^{-1}\mathbf{V}^H\right)^{-1} \\ &= \mathbf{V}\left(\mathbf{I}_{N_T} + \mu\mathbf{\Lambda}^{-1}\right)^{-1}\mathbf{V}^H \\ &= \mathbf{V}\mathbf{D}_\mu\mathbf{V}^H. \end{aligned} \tag{18}$$

Substituting (18) in (17), we obtain the expression in (12) for $\mathbf{p}$. Then, we have that if there exists μ such that $\|\mathbf{p}\|^2 = \varepsilon^2$, then $\mathbf{p}$ satisfies the KKT conditions and is therefore an optimal solution to (8). From (12), we have that $\|\mathbf{p}\|^2$ can be calculated as

$$\begin{aligned} \|\mathbf{e}\|^2 &= \|\mathbf{V}\mathbf{D}_\mu\mathbf{V}^H\mathbf{f}\|^2 \\ &= \|\mathbf{D}_\mu\mathbf{u}\|^2 \\ &= \sum_{n=1}^{N_T}\left(\frac{|u_n|}{1+\mu/\lambda_n}\right)^2, \end{aligned} \tag{19}$$

which gives the condition in (11). ■

To show the existence of μ satisfying (11), we define the function

$$h(\mu) = \sum_{n=1}^{N_t}\left(\frac{u_n}{1+\mu/\lambda_n}\right)^2. \tag{20}$$

The function $h(\mu)$ is clearly continuous and strictly monotone decreasing, and we have $h(0) = \|\mathbf{f}\|^2$ and $\lim_{\mu\to\infty} h(\mu) = 0$. Since $\varepsilon \in (0,\|\mathbf{f}\|)$, there exists $\mu_\varepsilon \in (0,\infty)$ for which $h(\mu_\varepsilon) = \varepsilon^2$, and μ_ε is the optimal dual variable for the optimization in (8) with perturbation size ε. From (11), we also have that μ_ε can be bounded by

$$\lambda_{N_t}\left(\frac{\|\mathbf{f}\|}{\varepsilon} - 1\right) \le \mu_\varepsilon \le \lambda_1\left(\frac{\|\mathbf{f}\|}{\varepsilon} - 1\right), \tag{21}$$

where λ_1 and λ_{N_t} are the largest and smallest eigenvalues of $\mathbf{R}$, respectively. Therefore, μ_ε can be found by simple a one-dimensional search method.

While it is clear that $\mathbf{f}_\varepsilon$ induces lower exposure than $\mathbf{f}$, it must satisfy both the power and the exposure constraint to be viable. For a given ε and a corresponding optimal dual variable μ_ε, the exposure induced by $\tilde{\mathbf{f}}_\varepsilon$ is given by

$$\tilde{\mathbf{f}}_\varepsilon^H\mathbf{R}\tilde{\mathbf{f}}_\varepsilon = \mathbf{u}^H\mathbf{\Lambda}\left(\mathbf{I} - \mathbf{D}_{\mu_\varepsilon}\right)^2\mathbf{u} \tag{22}$$

$$= \sum_{n=1}^{N_t}|u|^2\lambda_n\left(\frac{\mu_\varepsilon}{\lambda_n + \mu_\varepsilon}\right)^2. \tag{23}$$

Note that $\tilde{\mathbf{f}}_\varepsilon^H\mathbf{R}\tilde{\mathbf{f}}_\varepsilon$ can be reduced as desired by decreasing μ_ε, or, equivalently, by increasing ε. However, increasing the value of ε may result in a large perturbation to $\mathbf{f}$ and degrade the system performance. The optimal perturbation size ε^* is therefore defined as the smallest ε which results in an exposure compliant beamformer $\tilde{\mathbf{f}}_\varepsilon$ and is given by

$$\begin{aligned} \varepsilon^* = &\min \varepsilon \\ &s.t. \;\; \tilde{\mathbf{f}}_\varepsilon^H\mathbf{R}\tilde{\mathbf{f}}_\varepsilon \le Q. \end{aligned} \tag{24}$$

By definition, $\tilde{\mathbf{f}}_{\varepsilon^*}$ satisfies the exposure constraint. Additionally, the following Lemma shows that $\tilde{\mathbf{f}}_\varepsilon$ satisfies the power constraint for any $\varepsilon \in (0,\|\mathbf{f}\|)$ as long as $\mathbf{f}^H\mathbf{f} \le P$.

Lemma 3.2. *Let* $\tilde{\mathbf{f}}_\varepsilon = \mathbf{f} + \mathbf{p}_\varepsilon$*, where* $\mathbf{p}_\varepsilon$ *is the solution to* (8)*. Then* $\|\tilde{\mathbf{f}}_\varepsilon\| \le \|\mathbf{f}\|$.

Proof: Assume $\|\tilde{\mathbf{f}}_\varepsilon\| > \|\mathbf{f}\|$, and define $B : \mathbb{R} \to [0, \infty)$ by

$$B(t) = \|\mathbf{f} - t\tilde{\mathbf{f}}_\varepsilon\|^2 \tag{25}$$

$$= t^2 \tilde{\mathbf{f}}_\varepsilon^H \tilde{\mathbf{f}}_\varepsilon - 2t\text{Re}\left(\mathbf{f}^H \tilde{\mathbf{f}}_\varepsilon\right) + \mathbf{f}^H \mathbf{f}. \tag{26}$$

We have that $B(t)$ is a convex function since it is the restriction of the vector norm to a line. From convexity, the stationary point

$$t^* = \frac{\text{Re}\left(\mathbf{f}^H \tilde{\mathbf{f}}_\varepsilon\right)}{\tilde{\mathbf{f}}^H \tilde{\mathbf{f}}} \tag{27}$$

is a global minimum of $B(t)$. By assumption, t^* is bounded by

$$t^* \le \frac{|\mathbf{f}^H \tilde{\mathbf{f}}_\varepsilon|}{\tilde{\mathbf{f}}_\varepsilon^H \tilde{\mathbf{f}}_\varepsilon} \le \frac{\|\mathbf{f}\|}{\|\tilde{\mathbf{f}}_\varepsilon\|} < 1.$$

Also, we have

$$\begin{aligned} \text{Re}\left(\mathbf{f}^H \tilde{\mathbf{f}}_\varepsilon\right) &= \text{Re}\left(\mathbf{f}^H (\mathbf{f} + \mathbf{p}_\varepsilon)\right) \\ &\ge \mathbf{f}^H \mathbf{f} - |\mathbf{f}^H \mathbf{p}_\varepsilon| \\ &\ge \|\mathbf{f}\|^2 - \|\mathbf{f}\|\|\mathbf{p}_\varepsilon\| \\ &\ge \|\mathbf{f}\|^2 - \|\mathbf{p}_\varepsilon\|^2 \\ &> 0, \end{aligned} \tag{28}$$

which implies that $t^* > 0$. Since $B(1) = \varepsilon$, we have $B(t^*) \le \varepsilon$. Therefore, $\hat{\mathbf{p}}_\varepsilon = t^* \tilde{\mathbf{f}}_\varepsilon - \mathbf{f}$ is a feasible solution to (8). However, we have

$$(\mathbf{f} + \hat{\mathbf{p}}_\varepsilon)^H \mathbf{R} (\mathbf{f} + \hat{\mathbf{p}}_\varepsilon) = (t^*)^2 \tilde{\mathbf{f}}_\varepsilon^H \mathbf{R} \tilde{\mathbf{f}}_\varepsilon \tag{29}$$

$$< \tilde{\mathbf{f}}_\varepsilon^H \mathbf{R} \tilde{\mathbf{f}}_\varepsilon \tag{30}$$

$$= (\mathbf{f} + \mathbf{p}_\varepsilon)^H \mathbf{R} (\mathbf{f} + \mathbf{p}_\varepsilon), \tag{31}$$

which is a contradiction since $\mathbf{p}_\varepsilon$ is a solution to (8). Therefore, we must have $\|\tilde{\mathbf{f}}_\varepsilon\| \le \|\mathbf{f}\|$. ■

We denote $\mathbf{p}^* = \mathbf{p}_{\varepsilon^*}$ as the optimal perturbation, and generate the beamforming vector

$$\mathbf{f}_{\text{exp}} = \mathbf{f} + \mathbf{p}^* \tag{32}$$

for data transmission. As discussed above, $\mathbf{f}_{\mathsf{exp}}$ satisfies both the exposure constraint and the power constraint and therefore is a feasible solution to (4). The optimal perturbation vector can be found through two nested line searches, where the outer line search solves (24), and the inner line search solves (8) by finding μ_ε. These optimizations can be performed offline in codebook-based deployments. In this case, the proposed exposure-reducing scheme can be applied to construct a perturbed, exposure-compliant beamforming codebook.

The perturbation $\mathbf{f}_{\mathsf{exp}} = \mathbf{f} + \mathbf{p}^*$ can also be expressed as

$$\mathbf{f}_{\mathsf{exp}} = \alpha \mathbf{f} + \mathbf{e}, \tag{33}$$

where α is a constant and $\mathbf{e} = (1 - \alpha)\mathbf{f} + \mathbf{p}^*$ is orthogonal to $\mathbf{f}$, i.e, $\mathbf{e}^H \mathbf{f} = 0$. By using the expression for the perturbation vector given in (12), α can be calculated as

$$\alpha = 1 - \frac{\mathbf{u}^H \mathbf{D}_{\mu^*} \mathbf{u}}{\mathbf{u}^H \mathbf{u}}, \tag{34}$$

where μ^* is the dual variable obtained from solving (8) with perturbation size ε^*. One can see from (10) that the entries of $\mathbf{D}_\mu$ are in the interval $[0, 1]$ for any μ, which implies $\alpha \in [0, 1]$. Therefore, α can be interpreted as a power back-off factor acting on the main beam $\mathbf{f}$. The vector $\mathbf{e}$ directs power in a direction orthogonal to $\mathbf{f}$ to cancel out some of the exposure from $\mathbf{f}$. As shown in Section IV, doing so allows the system to beamform along $\mathbf{f}$ with higher power than that from adaptive power back-off.

The beamforming gain of $\mathbf{f}_{\mathsf{exp}}$ is given by

$$\|\mathbf{H}\mathbf{f}_{\mathsf{exp}}\|^2 = \alpha^2 \|\mathbf{H}\mathbf{f}\|^2 + 2\alpha \text{Re}\left(\mathbf{f}^H \mathbf{H}^H \mathbf{H} \mathbf{e}\right) \|\mathbf{H}\mathbf{e}\|^2. \tag{35}$$

If maximum ratio transmission (MRT) is applied to obtain $\mathbf{f}$, then $\mathbf{f}$ is the dominant right singular vector of $\mathbf{H}$, and the beamforming gain $\|\mathbf{H}\mathbf{f}_{\mathsf{exp}}\|^2$ can be bounded in terms of the original beamforming $\|\mathbf{H}\mathbf{f}\|^2$ as

$$\left\|\mathbf{H}\mathbf{f}_{\mathsf{exp}}\right\|^2 \ge \alpha^2 \|\mathbf{H}\mathbf{f}\|^2 = \alpha^2 \sigma_1, \tag{36}$$

where σ_1 is the largest singular value of $\mathbf{H}$. In general, however the beamforming gain of the proposed scheme can only be approximated as $\alpha^2 \|\mathbf{H}\mathbf{f}\|^2$.

IV. Simulation Results

In this section, we compare the performance of the proposed exposure reduction scheme with the traditional power back-off methods and the optimal solution to (4). We consider a MIMO system with $N_t = 2$ and $N_r = 2$. We performed Monte Carlo simulations with i.i.d. Rayleigh fading, where the entries of $\mathbf{H}$ are distributed according to $\mathcal{CN}(0, 1)$. The noise variance $\sigma^2 = 1$ in all simulations. We placed a SAR constraint on the system and used a SAR matrix obtained from [13] given by

$$\mathbf{R} = \begin{bmatrix} r_1 & r_2 e^{j\varphi} \\ r_2 e^{-j\varphi} & r_1 \end{bmatrix}, \tag{37}$$

where $r_1 = 4.6050$, $r_2 = 2.6250$, and $\varphi = 0.78\pi$. In all simulations, we fixed the SAR constraint to $Q = 1.6$ W/kg and varied the transmit power P.

In Fig. 2 the proposed exposure reduction scheme and the traditional back-off methods are applied to the MRT beamformer. The proposed method achieves better SNR than both of the traditional power back-off methods. At $P = 1$ W, the proposed method achieves a gain of 0.5 dB over the adaptive back-off method and falls only 1 dB short of the optimal method.

In Fig. 3, we plot the back-off factor for the adaptive power back-off scheme given in (6) and the back-off factor for the proposed scheme given in (34) for the case of MRT beamforming. The proposed scheme allows the systems to transmit with a higher power than the adaptive power scheme, resulting in the performance gains seen in Fig. 2.

In Fig. 4, we employ the uplink beamforming codebook from LTE Release 15 [19]. For a given channel, the system selects the codebook vector which achieves the largest beamforming gain and then applies the desired exposure mitigation strategy. Note that the optimal approach is not bound to the codebook vectors. The proposed method performs better than the power back-off schemes and demonstrates a gain of

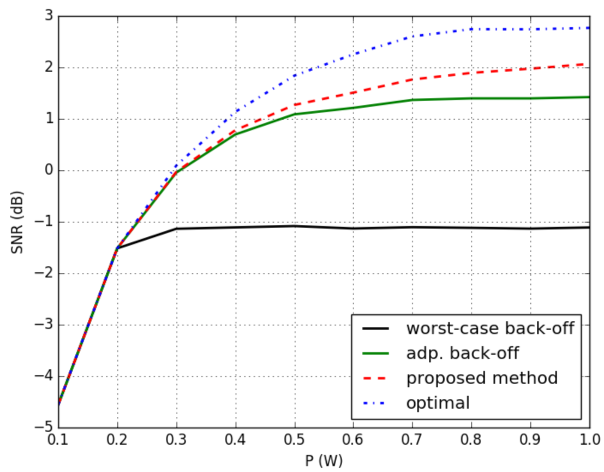

Fig. 2. Average receive SNR as a function of the transmit power P for a SAR-constrained 2x2 MIMO system. The proposed method and the power back-off methods are applied to the MRT beamformer. Our approach has a 0.5 dB gain over the adaptive back-off method at $P = 1$ W.

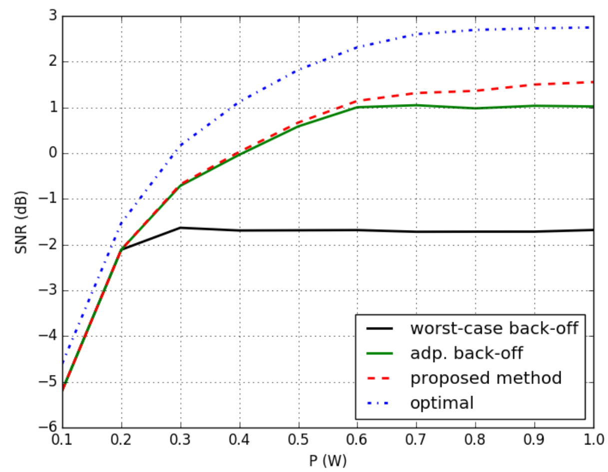

Fig. 4. Average receive SNR as a function of the transmit power P for a 2x2 MIMO system. The proposed method and the power back-off methods are applied to an LTE codebook from [19]. The proposed method achieves better performance than the two back-off methods.

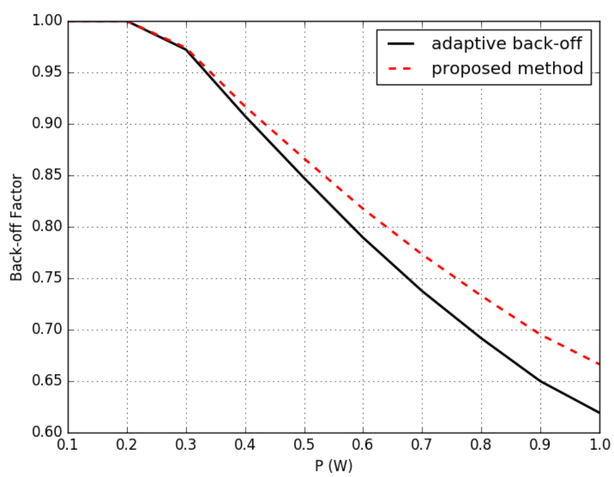

Fig. 3. The main beam back-off factor as a function of the transmit power P for a SAR-constrained 2x2 MIMO system. The adaptive back-off factor is given in (6) and the back-off factor for the proposed method is given in (34). By directing energy in a direction orthogonal to the main beam, the proposed method allows the system to beamform along the main beam with a higher power than the adaptive power back-off scheme.

approximately 0.5 dB over the adaptive back-off scheme when $P = 1$ W.

V. Conclusion

In this paper, we developed a low-complexity perturbation approach to reduce the exposure of a given beamforming vector in order to comply with exposure limits. The proposed method can be interpreted as reducing the power of the original beamformer and directing energy in an orthogonal direction to decrease exposure. By employing the proposed method, the system is able to direct more power in the original beamforming direction than when employing traditional power back-off methods. Simulation results demonstrate that the proposed method is able to outperform the simpler back-off methods, and only incurs a relatively small loss compared to the optimal exposure-aware beamforming approach.

References

[1] National Institutes of Health, National Cancer Institute, "Cell phones and cancer risk," Jan. 2019. [Online]. Available: https://www.cancer.gov/about-cancer/causes-prevention/risk/radiation/cell-phones-fact-sheet.

[2] FCC, "Electronic code of federal regulation, title 47 telecommunication, 2.1093 radiofrequency radiation exposure evaluation: portable devices," Tech. Rep., Aug. 2015.

[3] ICNIRP, "Guidelines for limiting exposure to time-varying electric, magnetic, and electromagnetic fields (up to 300 GHz)," *Health Phys.*, vol. 74, no. 4, pp. 494–521, Apr. 1998.

[4] T. Wu, T. S. Rappaport, and C. M. Collins, "Safe for generations to come: Considerations of safety for millimeter waves in wireless communications," *IEEE Microw. Mag.*, vol. 16, no. 2, pp. 65–84, Mar. 2015.

[5] *IEEE Standard for Safety Levels with Respect to Human Exposure to Radio Frequency Electromagnetic Fields, 3 kHz to 300 GHz.* IEEE Standard C95.1-2005, 2005.

[6] M. Zhadobov, N. Chahat, R. Sauleau, C. Le Quement, and Y. Le Drean, "Millimeter-wave interactions with the human body: state of knowledge and recent advances," *Int. J. Microw. Wirel. Technol.*, vol. 3, no. 02, pp. 237–247, Apr. 2011.

[7] S. Hur, T. Kim, D. J. Love, J. V. Krogmeier, T. A. Thomas, and A. Ghosh, "Millimeter wave beamforming for wireless backhaul and access in small cell networks," *IEEE Trans. Commun.*, vol. 61, no. 10, pp. 4391–4403, Oct. 2013.

[8] C. Dehos, J. L. González, A. De Domenico, D. Ktenas, and L. Dussopt, "Millimeter-wave access and backhauling: the solution to the exponential data traffic increase in 5G mobile communications systems?" *IEEE Commun. Mag.*, vol. 52, no. 9, pp. 88–95, Sept. 2014.

[9] J. Li, S. Yan, Y. Liu, B. M. Hochwald, and J.-M. Jin, "A high-order model for fast estimation of electromagnetic absorption induced by multiple transmitters in portable devices," *IEEE Trans. Antennas Propag.*, vol. 65, no. 12, pp. 6768–6778, Dec. 2017.

[10] A. Ebadi-Shahrivar, J. Ren, B. M. Hochwald, P. Fay, J.-M. Jin, and D. J. Love, "Mixed quadratic model for peak spatial-average SAR of coherent multiple antenna devices," in *Proc. IEEE Int. Symp. Antennas and Propagation USNC/URSI Nat. Radio Science Meeting*, San Diego, CA, USA, July 2017, pp. 1419–1420.

[11] B. M. Hochwald, D. J. Love, S. Yan, P. Fay, and J.-M. Jin, "Incorporating specific absorption rate constraints into wireless signal design," *IEEE Commun. Mag.*, vol. 52, no. 9, pp. 126–133, Sept. 2014.

[12] B. M. Hochwald, D. J. Love, S. Yan, and J. Jin, "SAR codes," in *UCSD Information Theory Appl. Workshop (ITA)*, San Diego, CA, USA, Feb. 2013, pp. 1–9.

[13] B. M. Hochwald and D. J. Love, "Minimizing exposure to electromagnetic radiation in portable devices," in *UCSD Information Theory Appl. Workshop (ITA)*, San Diego, CA, USA, Feb. 2012, pp. 255–261.

[14] A. Ebadi-Shahrivar, P. Fay, B. M. Hochwald, and D. J. Love, "Multi-antenna SAR estimation in linear time," in *Proc. IEEE AP-S Int. Symp. Antennas and Propagation USNC/URSI Nat. Radio Science Meeting*, Boston, MA, USA, July 2018, pp. 583–584.

[15] A. Ebadi-Shahrivar, P. Fay, D. J. Love, and B. M. Hochwald, "Determining electromagnetic exposure compliance of multi-antenna devices in linear time," accepted in *IEEE Trans. Antennas Propag.*, Apr. 2019.

[16] D. Ying, D. J. Love, and B. M. Hochwald, "Closed-loop precoding and capacity analysis for multiple antenna wireless systems with user radiation exposure constraints," *IEEE Trans. Wireless Commun.*, vol. 14, no. 10, pp. 5859–5870, Oct. 2015.

[17] D. Ying, D. J. Love, and B. M. Hochwald, "Sum-rate analysis for multi-user MIMO systems with user exposure constraints," *IEEE Trans. Wireless Commun.*, vol. 16, no. 11, pp. 7376–7388, Sept. 2017.

[18] M. R. Castellanos, D. Ying, D. J. Love, B. Peleato, and B. M. Hochwald, "Dynamic electromagnetic exposure allocation for rayleigh fading MIMO channels," submitted to *IEEE Trans. Wireless Commun.*, June 2019.

[19] 3GPP TS 36.211, "Evolved universal terrestrial radio access (E-UTRA); Physical channels and modulation," (Release 15).